Supporting Information

Dual Z-Scheme g-C_3N_4/GQDs/$ZnIn_2S_4$ Composite with Enhanced Photocatalytic Degradation of Xanthate under Visible Light Irradiation

Yunpei Cui[a,b,c,1], Hangyu Shi[b,c,1], Shuangshuang Zuo[b,c], Jiewei Xie[b,c], Hua Cao[c], Lei Yang[c,d], Qianqian Nie[a]*, Hesheng Yu[b,c,d]*

a. School of Physics and New Energy, Xuzhou University of Technology, Xuzhou, Jiangsu 221018, China

b. State Key Laboratory of Coking Coal Resources Green Exploitation, China University of Mining and Technology, Xuzhou, Jiangsu 221116, China

c. School of Chemical Engineering and Technology, China University of Mining and Technology, Xuzhou, Jiangsu, 221116, China

d. College of Mining and Geology, Xinjiang Institute of Engineering, Urumqi, Xinjiang 830023, China

1. These authors contribute equally.

* Corresponding Authors:

Dr. Qianqian Nie, School of Physics and New Energy, Xuzhou University of Technology, Xuzhou, Jiangsu 221018, China. E-mail: nieqq@xzit.edu.cn

Dr. Hesheng Yu, School of Chemical Engineering and Technology, China University of Mining and Technology, Xuzhou, Jiangsu, 221116, China. E-mail: heshengyu@cumt.edu.cn

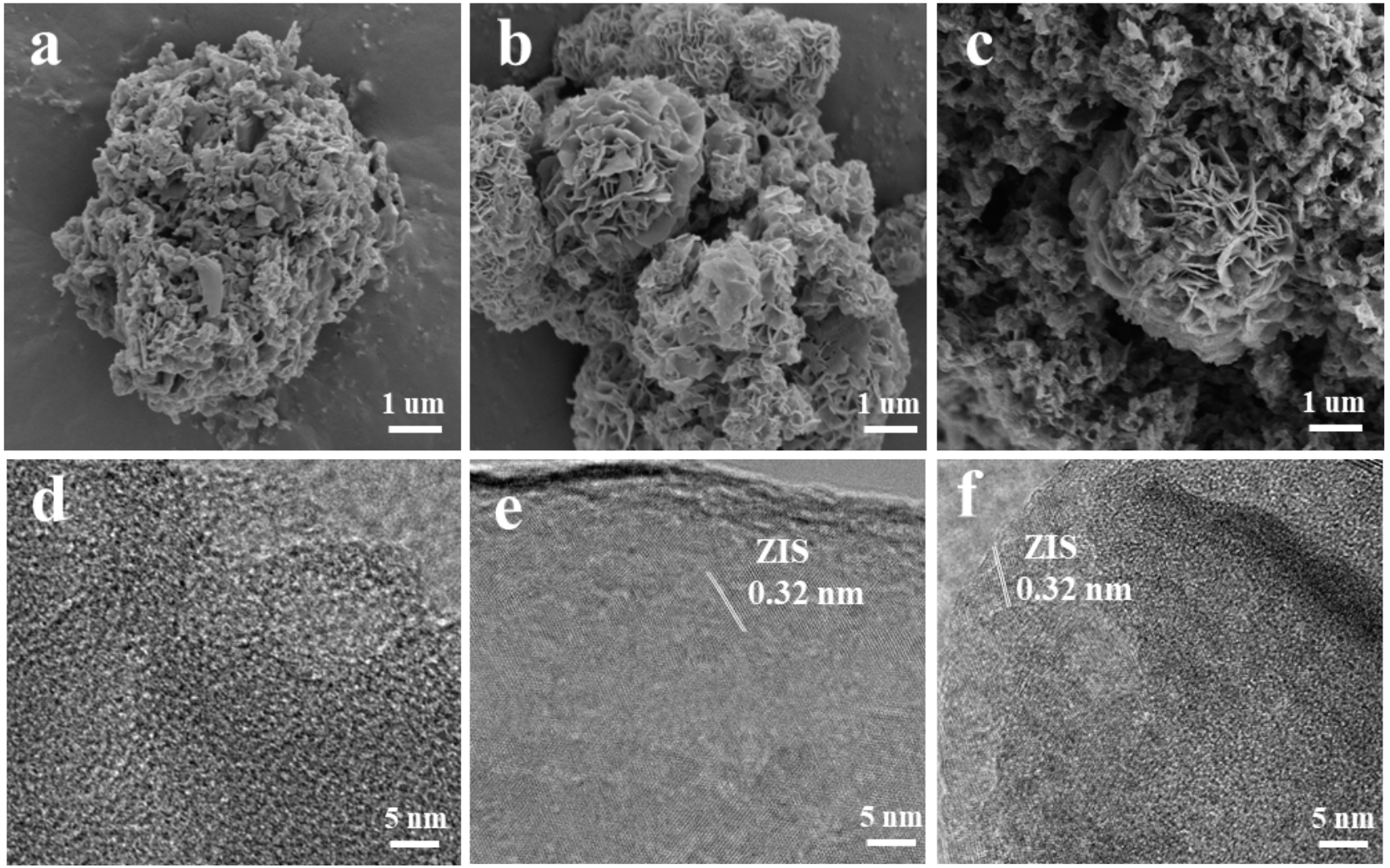

Fig. S1 FE-SEM image of (a) CN; (b) ZIS; and (c) CN/ZIS; HR-TEM images of (d) CN; (e) ZIS; and (f) CN/ZIS.

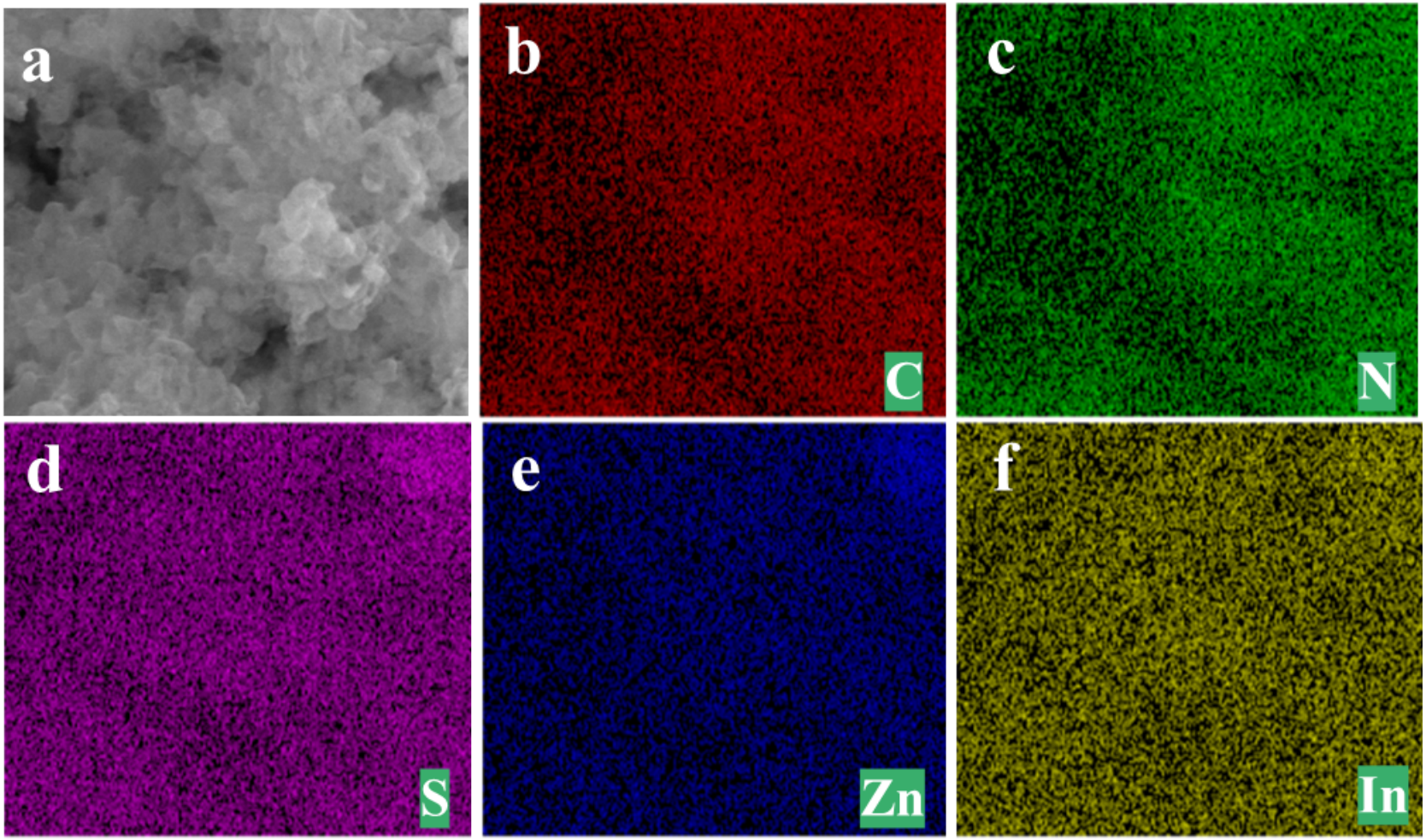

Fig. S2 (a) FE-SEM image of CN/50GQDs/ZIS; EDS mapping images of (b)C; (c)N; (d)S; (e)Zn; and (f) In of CN/50GQDs/ZIS.

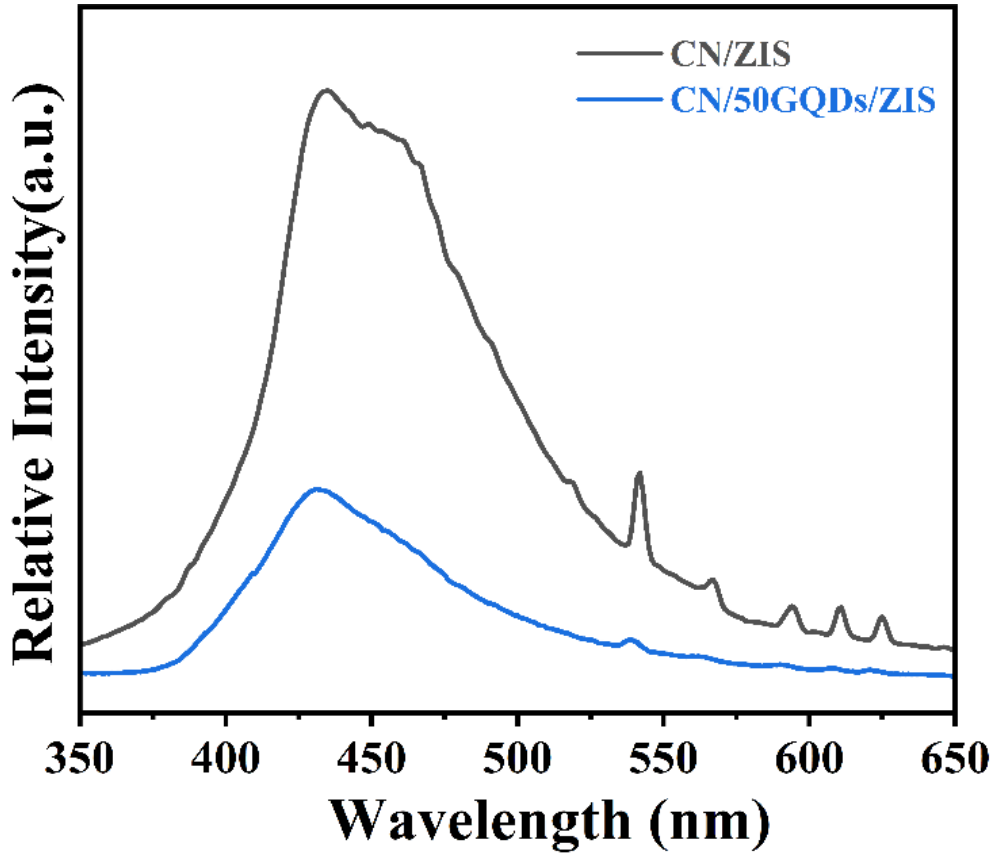

Fig. S3 PL spectra of CN/ZIS and CN/50GQDs/ZIS.

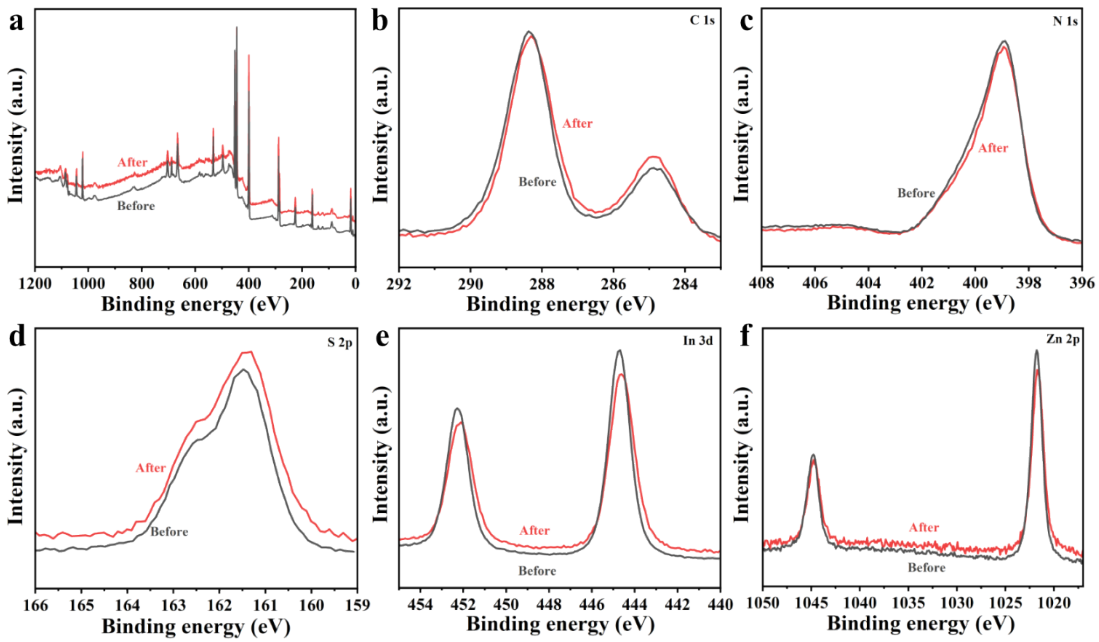

Fig. S4 XPS spectra of CN/50GQDs/ZIS before and after the cycling test: (a) survey spectrum, and high-resolution spectra of (b) C 1s, (c) N 1s, (d) S 2p, (e) In 3d, and (f) Zn 2p.

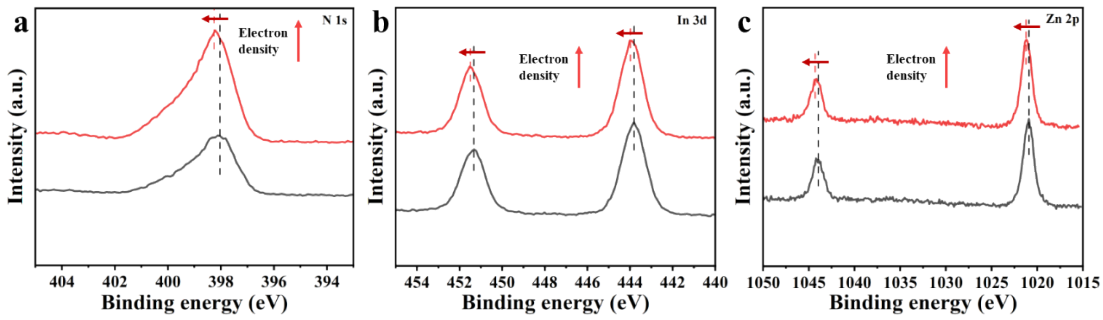

Fig. S5 *In situ* irradiated XPS spectra of CN/50GQDs/ZIS recorded under dark conditions and after 15 min visible-light irradiation: (a) N 1s, (b) In 3d, and (c) Zn 2p.

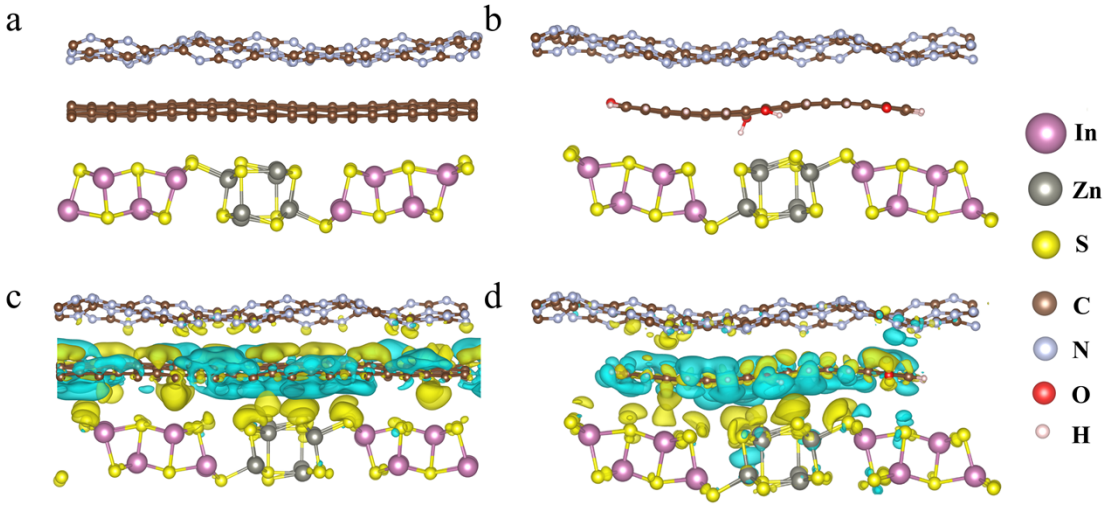

Fig. S6 Structural and electrostatic potential characteristics of CN/graphene/ZIS and CN/GQDs/ZIS heterojunctions: (a, b) Structural diagrams of CN/graphene/ZIS and CN/GQDs/ZIS, respectively; (c, d) Electrostatic potential distributions at the heterojunction interfaces for the two systems, respectively.

The UV-Vis diffuse reflectance spectra were transformed using the Kubelka–Munk function:

$$F(R_\infty) = \frac{(1 - R_\infty)^2}{2R_\infty} = \frac{K^*}{S} \qquad \textbf{S1}$$

where R_∞ is the absolute reflectance of an optically thick layer, and K^* and S are the Kubelka–Munk absorption and scattering coefficients, respectively. For powder samples, R_∞ is commonly approximated by the measured reflectance R. If S is weakly dependent on wavelength, $F(R)$ is proportional to the effective absorption, enabling

optical-gap evaluation from the corresponding plots.

Table S1 The data recorded for calculating the mass fraction of GQDs. [1]

	Volume (mL)	Tube weight (g)	GQDs and Tube weight (g)	GQDs weight (g)	Mass Ratio (mg/mL)
Solution 1	38.4	13.7534	13.8105	0.0571	1.487
Solution 2	41.0	14.0786	14.1320	0.0534	1.302
Solution 3	40.3	13.9625	14.0152	0.0527	1.308
		Average			1.366

note: **Table S1** Quantitative determination of the GQDs stock-solution concentration by the weight-difference method (reproduced from our previous work with the same preparation/purification procedure, with permission from Elsevier).

Table S2 Elemental analysis results of CN/ZIS and CN/50GQDs/ZIS composites

Samples	N(%)	C(%)	C/N
CN/ZIS	35.56	19.24	0.54
CN/50GQDs/ZIS	41.47	23.34	0.56

Reference

1. Y. P. Cui, X. X. Huang, T. Wang, L. H. Jia, Q. Q. Nie, Z. C. Tan and H. S. Yu, Carbon, 2022, 191, 502-514.